A Hybrid Control of Seismic Response by Passive and Semi-active Control Strategies

Res.Asist. Gökçe KINAY[1], Asist.Prof. Gürsoy TURAN[2]

[1]Mechanical Engineering Department, İYTE, İzmir, Turkey

gokcekinay@iyte.edu.tr

[2]Civil Engineering Department, İYTE, İzmir, Turkey

gursoyturan@iyte.edu.tr

KEYWORDS

MR damper, Hybrid control, Base isolation

ABSTRACT

Passive and semi-active control devices are widely utilized as supplemental damping strategies for response reduction in civil engineering structures subjected to strong earthquakes and severe winds. Passive control devices require no external power supply. Total energy cannot increase, therefore the system stays stable. But passive controllers are not as effective as semi-active, active, or hybrid ones. Semi-active control devices' input power requirements are negligible when compared to active devices. This fact makes semi-active controllers useful in case of a power cut during an earthquake. Active control strategies, on the other hand, are generally more effective, but they are disadvantageous as they need large amounts of power while they are in action, and they may result in instabilities of the controlled structure. A hybrid control which consists of passive and semi-active controllers is studied in order to benefit from advantages of both strategies and to compensate their weak properties. In the current study, a passive base isolator and a semi-active magnetorheological damper are applied to a three-story frame structure. The benefits of hybrid application of two control systems are revealed. The control method is based on the theory of linear quadratic regulator (LQR). The results are compared with respect to a base isolated structure. The structural responses are satisfactory moreover the isolator is protected from detrimental effects of the ground excitation. The interstory drift reduction at the base level when compared to the response of the base isolated structure is approximately 50%. As a result the base displacements and velocities are reduced by additional damping in the base level. Thus the base isolators are protected. On the other hand, the superstructure's responses increase due to the presence of large damping in the base level.

1. Introduction

Structural control may be utilized to reduce the amount of energy transferred into the structure from the ground motion either by using external energy or by absorbing a portion of the seismic energy. There exist passive, semi-active, active, and hybrid structural control systems [14]. In the present study, the attention is focused on a hybrid one due to the fact that it contains advantages of both of its components and it compensates weak properties of both components.

Semi-active control devices offer the versatility and adaptability of active devices without requiring large power sources and also offer the reliability of passive devices. Therefore they have become popular. Semi-active control devices in civil engineering applications are variable orifice dampers, friction controllable braces, friction controllable isolators, variable stiffness devices,and controllable fluid dampers which utilize electrorheological or magnetorheological fluids. Variable orifice (Vo) dampers are hydraulic dampers, whose damping coefficient can be changed by mechanically adjusting a valve. Magnetorheological (MR) dampers are semi-active control devices that utilize MR fluids to produce controllable damping forces [7].

Some advantages of MR dampers are their low power requirements, high yield strength that allows large force capacity, low viscosity, and stable hysteretic behavior over a wide temperature range. The most attractive property of the controllable MR fluids is their ability to reversibly change from a free-flowing, linear viscous fluid to a semi-solid with a controllable yield strength in milliseconds when exposed to an magnetic field [12].

Passive base isolation systems are currently more adopted in the control technology than semi-active MR dampers. There exist two types of base isolation, namely, the elastomeric-based systems and sliding-base systems. The elastomeric-based systems can be divided into two: low-damping rubber bearings and lead-core bearings.

The main idea of base isolation is that the structure is mounted on a suitably flexible base such that the high frequency component of ground motion is filtered out and the fundamental vibration period is lengthened. This results in deformation in the isolation system only, thus keeping the structure above almost unaffected. However, if the earthquake excitation contains a major component of this fundamental period, there will be large sidesway motions, both in the isolator and superstructure[1].

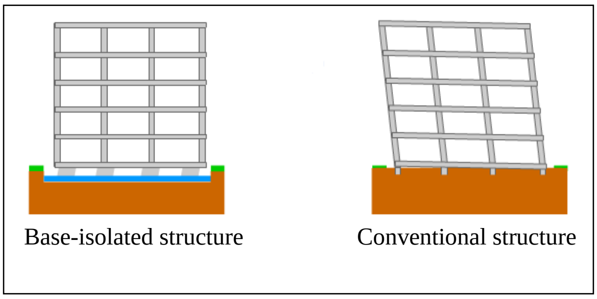

Figure 1. Responses of a base-isolated and a conventional structure under seismic excitation [1]

Passive supplemental damping in a seismically isolated structure provides the necessary energy dissipation to limit the isolation system displacement. However, damper forces can become quite large as the passive damping level is increased. Utilization of an intelligent hybrid control system containing semi-active damper in which the damping coefficient can be modulated is a possible solution to limit the level of damping force while simultaneously controlling the isolation system displacement [14].

In the current research, a hybrid control system which consists of a semi-active MR damper in parallel to a base isolation system is studied. The MR damper is activated only when the base drift exceeds 5 centimeters.

2. Semi-Active Magnetorheological Damper

The behaviour of magnetorheological dampers are highly nonlinear. Different phenomenological models exist in the literature for MR fluids. In the current work the modified Bouc-Wen model proposed by Spencer et al. is utilized. It is composed of Bouc-Wen hysteresis, springs, and dashpots to accurately reproduce the MR damper behavior.

A modified clipped-optimal control strategy is utilized to control the MR damper. The controller consists of a linear optimal control part and a modified clipped algorithm.

3. Modified Clipped Optimal Control

In the present work a modified clipped optimal control algorithm is utilized to determine the desired control forces [16]. In the optimal control algorithm, control signals that will cause the system to satisfy some physical constraints and at the same time maximize or minimize a chosen performance criteria (cost function) are determined. The block diagram of the semi-active control system is presented in Fig.2.

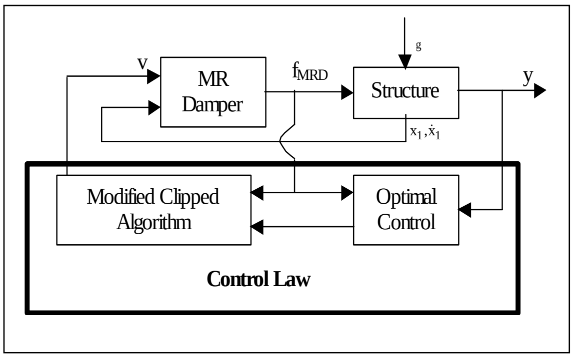

Figure 2. Block diagram of the semi-active control system

By choosing the optimal control algorithm, control signals that will cause the system to satisfy some physical constraints and at the same time maximize or minimize a chosen performance criteria (cost function) are determined. A linear optimal controller $\mathbf{K}_c$ is designed in order to provide the optimal control force u_c based on the states **x** which are the story displacements and velocities. The linear quadratic regulator (LQR) computes an optimal control u_c = - $\mathbf{K}_c$ **x** to stabilize the plant and to minimize a cost function given by

$$J = \int_0^{\infty} (\mathbf{x}^T \mathbf{Q}\,\mathbf{x} + u_c^{\ T} R u_c)dt \qquad (1)$$

where **Q** and R are weights of states and control. The optimal control is given by

$$u_c = -R^{-1}\mathbf{B}^T P\,\mathbf{x} \qquad (2)$$

where P is the solution of the algebraic Riccati equation given in (3). **A** and **B** matrices are the system matrices in state space representation.

$$\mathbf{A}^T P + P\mathbf{A} + \mathbf{Q} + P\mathbf{B}R^{-1}\mathbf{B}^T P = \mathbf{0} \qquad (3)$$

In the present work, the off-diagonal terms of **Q** matrix are zero emphasizing the uncoupled nature of degrees of freedom in the present problem. The diagonal terms of **Q** matrix are [0.061 0.0061 0.0061 0.0061 0.1833 0.0183 0.0183 0.0183]. The weight of the base responses are ten times higher than the floor responses'. The R value in the current research is 1e-8. R should be strictly positive definite. Note that the important issue in LQR is not the individual values of **Q** and R but the ratio between them.

The magnetic field in the damper is set by a modified clipped controller to develop damping forces that are equal to those obtained by the optimal control. The MR damper is driven by the magnetic field around it, hence driven by the voltage applied to the electromagnet. The applied voltage is set by a clipped algorithm to obtain the desired forces by the MR damper.

4. Passive Base Isolation

The base mass is chosen as 1.5 times the storey mass. 4 per cent damping is determined for base. The base period is chosen as 30 times the fundamental period of the superstructure leading to 5.5 seconds. The stiffness and damping factors are calculated by

$$k_b = (3m + m_b)\omega_b^2 \quad \text{and} \quad c_b = 2\xi_b(3m + m_b)\omega_b \qquad (4)$$

where m and m_b are masses of stories and base respectively [8,9,13]. ω_b is the base frequency. ξ_b is the base damping coefficient.

Additionally, a hybrid control system which is constituted from passive base isolator and MR damper is designed [2,4,5]. The MR damper is mounted to the base level in order to avoid the isolator to yield [11]. The MR damper is activated only when the base drift exceeds 50 per cent of the isolator's displacement capacity, which is chosen to be 5 centimeters.

5. Numerical Simulations

The model structure has three-stories and one base. MR damper is rigidly attached between the base and the ground. The model structure is given in Fig.3.

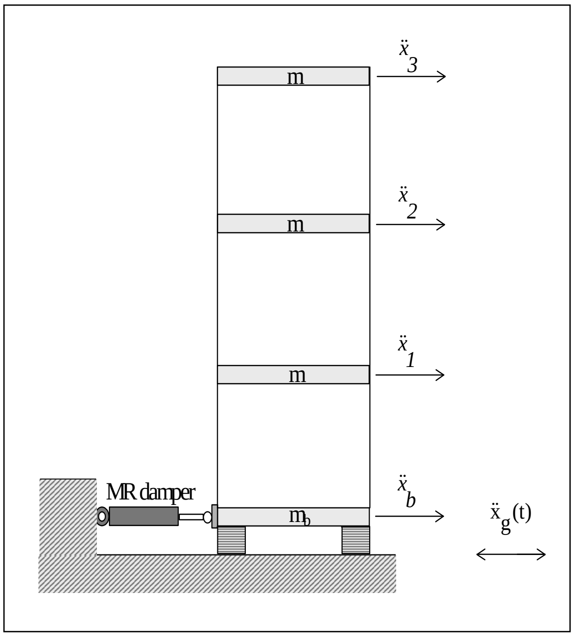

Figure 3. Model structure

The equations of motion for the whole system remaining in the linear region is given by

$$\mathbf{M}^*\ddot{\mathbf{x}}^* + \mathbf{C}^*\dot{\mathbf{x}}^* + \mathbf{K}^*\mathbf{x}^* = -\mathbf{\Gamma}^* f_{MRD} - \mathbf{M}^*\mathbf{\Lambda}^*\ddot{x}_g \quad (5)$$

where

$$\mathbf{M}^* = \begin{bmatrix} m_b & 0 & 0 & 0 \\ 0 & m_1 & 0 & 0 \\ 0 & 0 & m_2 & 0 \\ 0 & 0 & 0 & m_3 \end{bmatrix}, \quad \mathbf{C}^* = \begin{bmatrix} c_b + c_1 & -c_1 & 0 & 0 \\ -c_1 & c_1 + c_2 & -c_2 & 0 \\ 0 & -c_2 & c_2 + c_3 & -c_3 \\ 0 & 0 & -c_3 & c_3 \end{bmatrix} \quad (6)$$

and

$$\mathbf{K}^* = \begin{bmatrix} k_b + k_1 & -k_1 & 0 & 0 \\ -k_1 & k_1 + k_2 & -k_2 & 0 \\ 0 & -k_2 & k_2 + k_3 & -k_3 \\ 0 & 0 & -k_3 & k_3 \end{bmatrix}, \quad \mathbf{\Gamma}^* = \begin{bmatrix} 1 \\ 0 \\ 0 \\ 0 \end{bmatrix}, \quad \mathbf{\Lambda}^* = \begin{bmatrix} 1 \\ 1 \\ 1 \\ 1 \end{bmatrix} \quad (7)$$

with m_b=147.5 kg, m_1=m_2=m_3= 98.3 kg, c_b=44 Ns/m, c_1=125 Ns/m, c_2=c_3=50 Ns/m, k_b=686 N/m, k_1=700 kN/m, k_2=k_3=684 kN/m. Here m,c and k stand for the mass, for the damping and for the stiffness of the base and of the floors.

$\mathbf{M}^*$, $\mathbf{C}^*$, $\mathbf{K}^*$ are the mass, damping, and stiffness matrices of the whole structure, respectively. f_{MRD} is the force generated by the MR damper. $\mathbf{\Gamma}^*$ and $\mathbf{\Lambda}^*$ are the location matrices of the control force and of the external excitation. They specify how the control force f_{MRD} and the ground excitation $\ddot{x}_g$ enter into the system. The base displacement x_b and the floor displacements x_i's (i=1,2,3) are relative to the ground.

The seismic data belong to the North-South component of the Imperial Valley 1940 earthquake El Centro station [10]. The original acceleration data is given in time and frequency domain in Fig.4(a) and Fig.4(b), respectively. The original earthquake acceleration data is zero-padded to 60 seconds in the numerical simulations in order to see the unforced response of the base. Additionally the earthquake acceleration is multiplied by a factor of 1.5 in order to apply a higher peak ground acceleration (PGA) value. The original data's PGA value is 0.31g.

The periods of the superstructure are 0.17, 0.06, 0.04 seconds. The periods become 5.05, 0.11, 0.06, 0.04 seconds by combining the base isolator. The structure becomes softer. A value for the isolator period was chosen such that the structure is pushed to the right towards the smaller magnitude ranges on the acceleration spectra. In the present research the structure is pushed to the smaller magnitude's range by means of the isolator period (Fig.4(b)). Hence the structure is protected from the detrimental effects of earthquake excitation. The fixed base and seismic isolated base structures' fundamental periods are marked by blue and green lines in Fig.4(b), respectively.

.

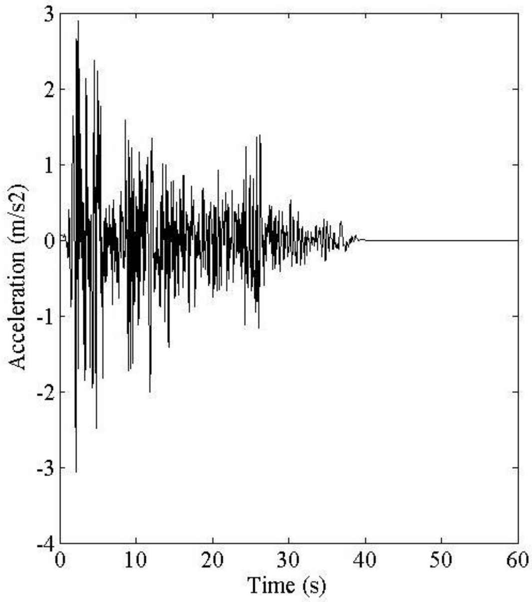

(a)

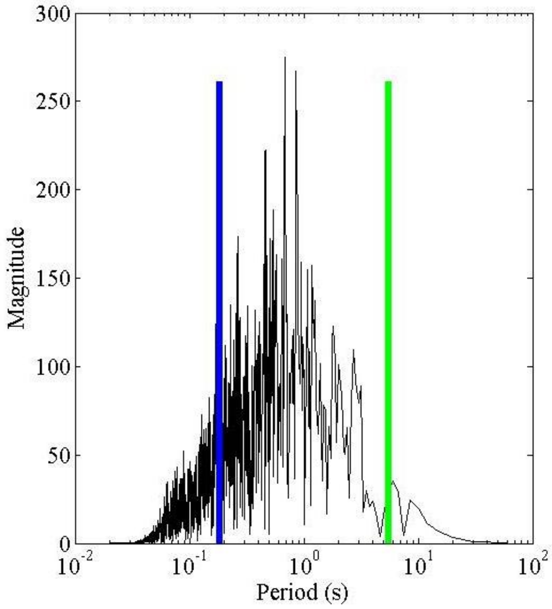

(b)

Figure 4. North-South component of the Imperial Valley 1940 earthquake El Centro station (a) in time and (b) in frequency domain

The base's interstory displacement, interstory velocity, and absolute acceleration values are presented in Fig.5. As it can be seen from the displacement time series, the MR damper is activated after the base drift exceeds 5 centimeters in the hybrid controlled case. The significance of the hybrid controller can be observed after the ground acceleration peaks at 25-28 seconds. The base isolated structure performs large deformation and the isolators would be damaged. On the other hand, the hybrid controller protects the base from large displacement and velocity responses. The absolute acceleration peak value reaches to 2g where g is the gravitational acceleration and it is a considerable value comparing to the benefit in displacements and velocities. The increase in accelerations is due to the fact that the damper adds energy to the structure at the base level.

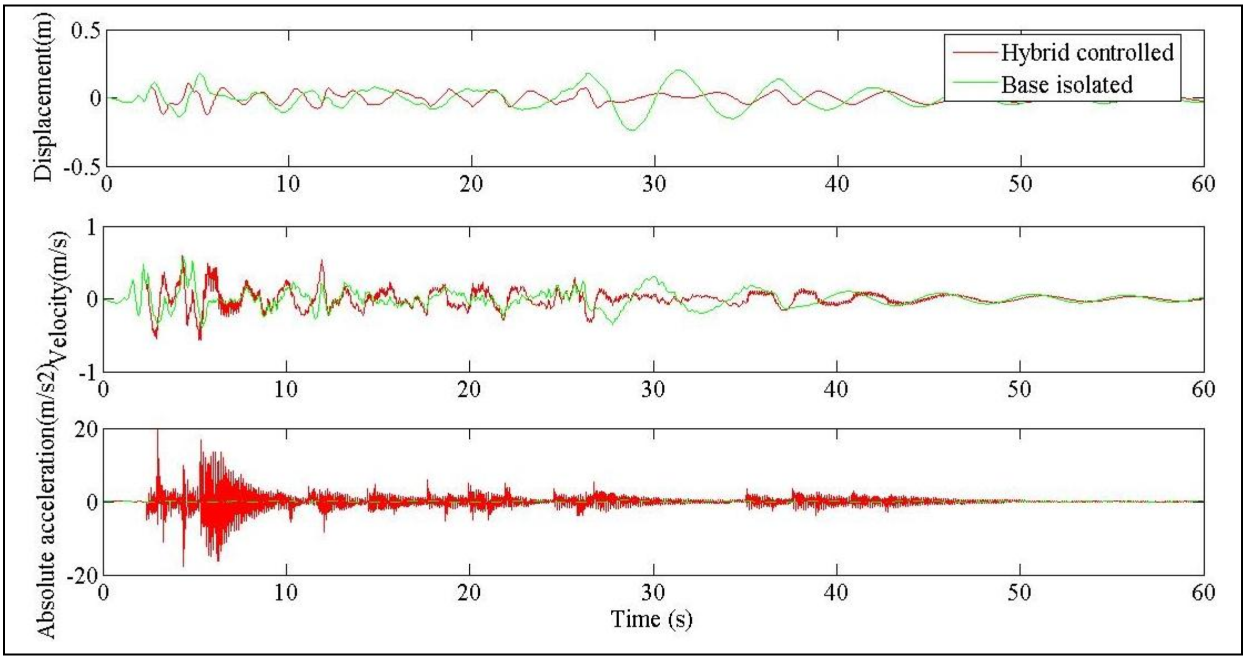

Figure 5. Interstory displacement, interstory velocity, and absolute acceleration responses of base floor in time domain

The hybrid controlled model structure's interstory displacement, interstory velocity, and absolute acceleration values for the first and third floors are presented in Fig.6 and Fig.7, respectively.

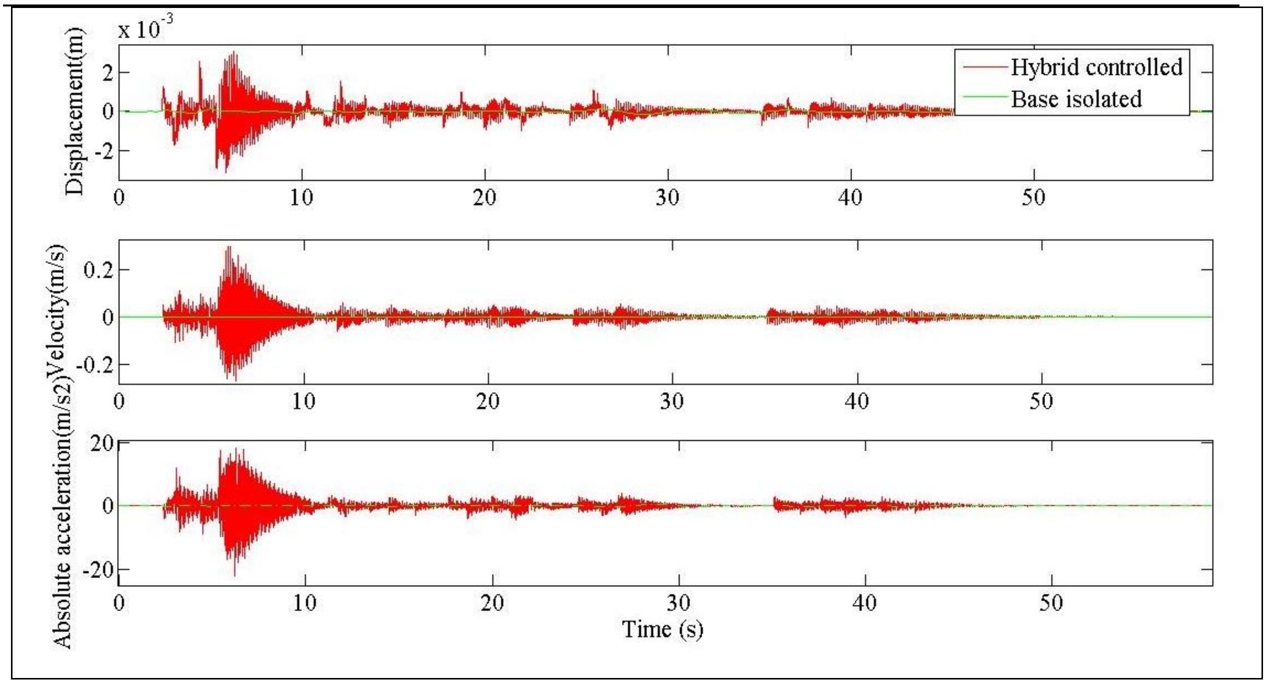

Figure 6. Interstory displacement, interstory velocity, and acceleration responses of the first floor in time domain

As it can be seen from the graphs, the floor responses are larger compared to the base isolated case. But the floor responses of the hybrid controlled structure are still in acceptable ranges (< 3.5 mm). This is an expected result which fact was taken into account during the engineering design.

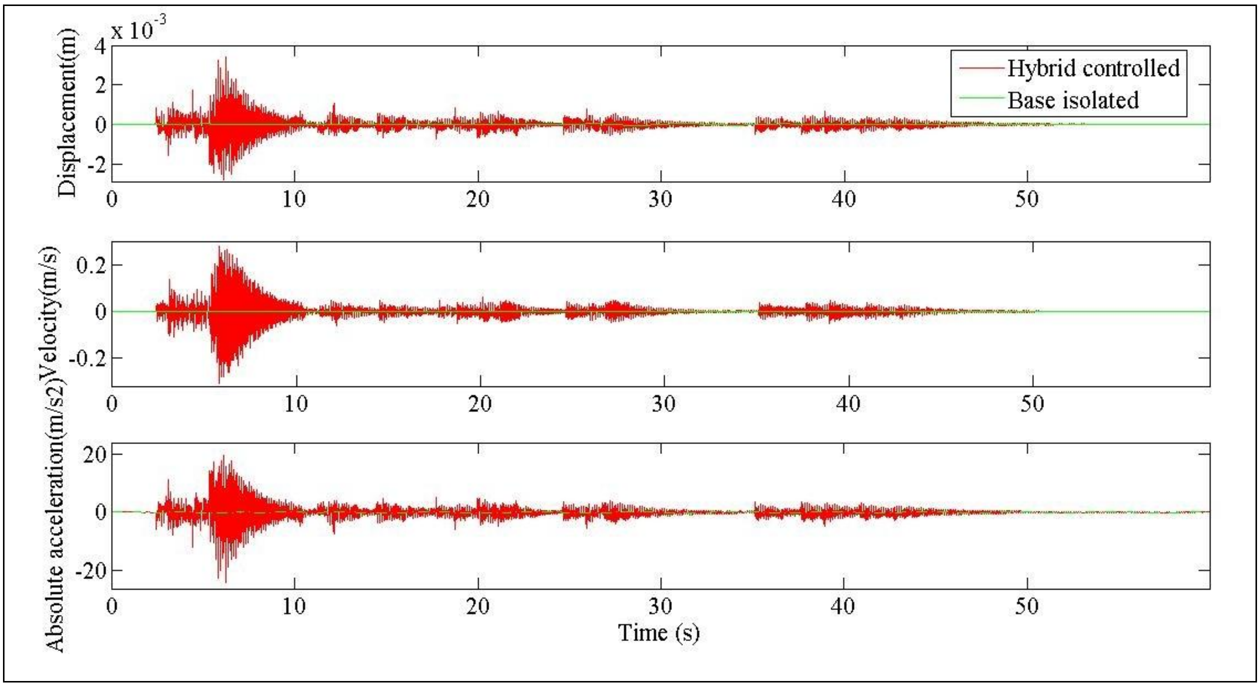

Figure 7. Interstory displacement, interstory velocity, and acceleration responses of the third floor in time domain

The displacement time histories of the ground, of the seismic isolated base, and of the hybrid controlled base are given in Fig.8. The values of the base are relative to the ground. Since the isolators are very soft, their relative displacements with respect to ground are almost equal to the negative value of the eartquake’s displacement, at least for the first two seconds. At time t=22 seconds, the ground moves at a period of approximately 6 seconds, which is close to the fundamental period of the isolated structure, for a total duration of approximately 12 seconds. Hence the structure gets into resonance, causing large structural displacements. The isolated structure has low damping resulting in large amplitude harmonic motion with a small decay. On the other hand, the amplitude for the hybrid controlled structure is approximately 50% smaller.

In theory, if the isolator can perform a relative displacement similar to the ground, then a small amount of displacement will remain for the superstructure. This is possible by choosing relatively high periods for isolators to rescue the structure from the range of low period excitations. In other words, the isolator acts as a low pass filter.

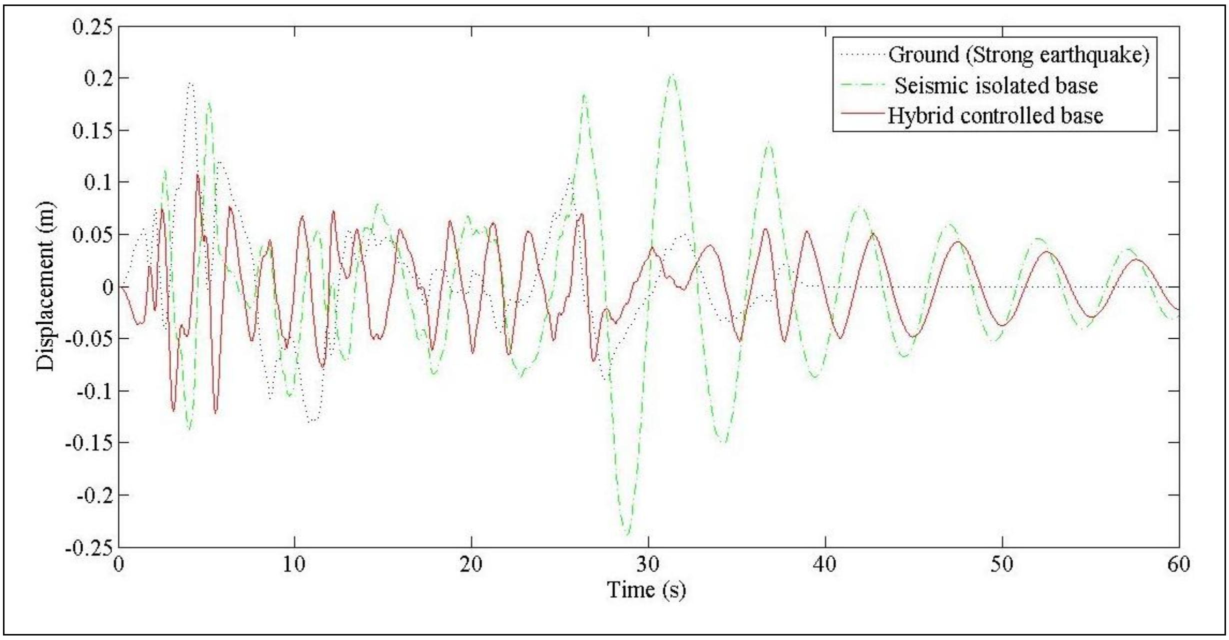

Figure 8**.** Displacement time histories of ground, of seismic isolated base and of hybrid controlled base (The values of the base are relative to the ground.)

The green dot-dashed line belong to the passive controlled system and red solid one is for the hybrid system. The beneficial effect of hybrid system can be easily seen. In the absence of MR damper the base's displacements are much higher and are damped out in a much larger period of time.

The maximum values of the responses of the base isolated and of the hybrid controlled structure are given in Table 1. By adding extra damping (MR damper) to the structural control system a reduction of 50% in terms of base displacement is obtained while the floor displacements which are still in acceptable range increase.

Table 1:Maximum values of the responses of the base isolated and of the hybrid controlled structure

	Base isolated structure			Hybrid controlled structure		
	Interstory displacement (m)	Interstory velocity (m/s)	Absolute acceleration (m/s^2)	Interstory displacement (m)	Interstory velocity (m/s)	Absolute acceleration (m/s^2)
Base	0.2384	0.58	0.37	0.1222	0.60	19
1st floor	0.0002	0.0008	0.37	0.0032	0.30	22
2nd floor	0.0001	0.0007	0.37	0.0027	0.19	18
3rd floor	0.00005	0.0005	0.37	0.0034	0.31	24

The interstory drifts of the first and of the third floors in frequency domain are given in Fig.9 and 10, respectively. As it is expected, the uncontrolled structure's response is driven mainly by the first mode. The second mode exhibits a smaller contribution to the response. On the other hand, the base isolated structure's response is driven by its fundamental mode and the effect of the other modes on the response can not be observed.

When the MR damper is added to the structure in addition to the base isolation, the first mode's period is slightly shortened and the contribution of the second and third modes have a larger effect at this time than the first mode. The frequency domain plots of the responses confirm the remarks that are made for the time domain responses.

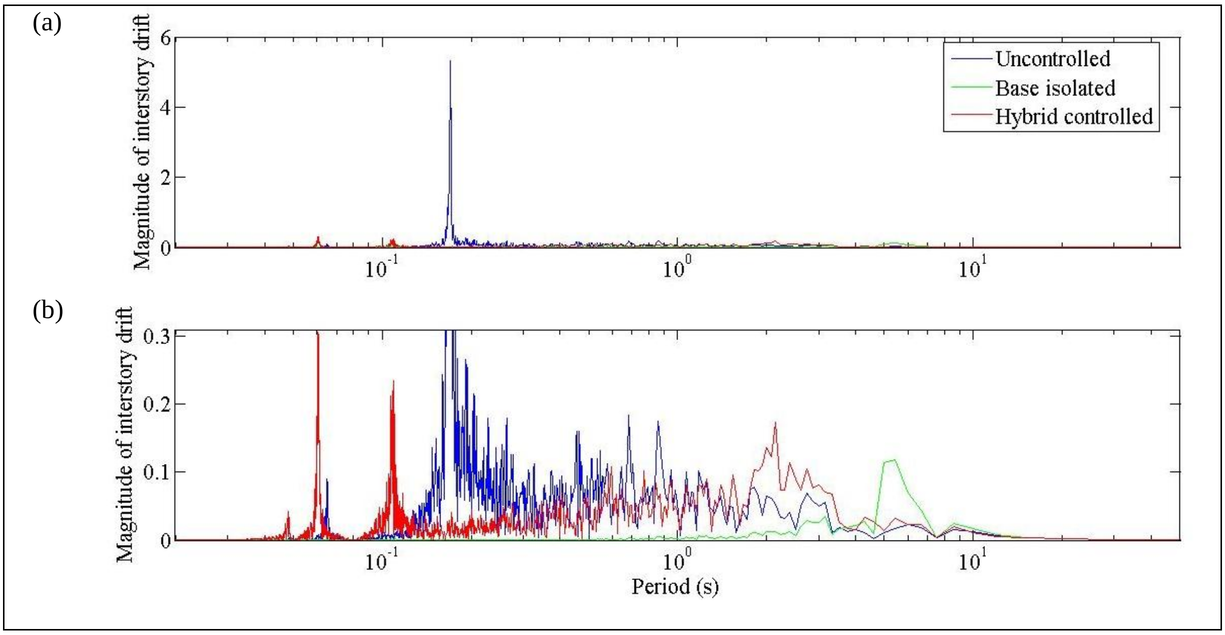

Figure 9. Interstory drift of the first floor in frequency domain ((b) is zoomed in vertical axis.

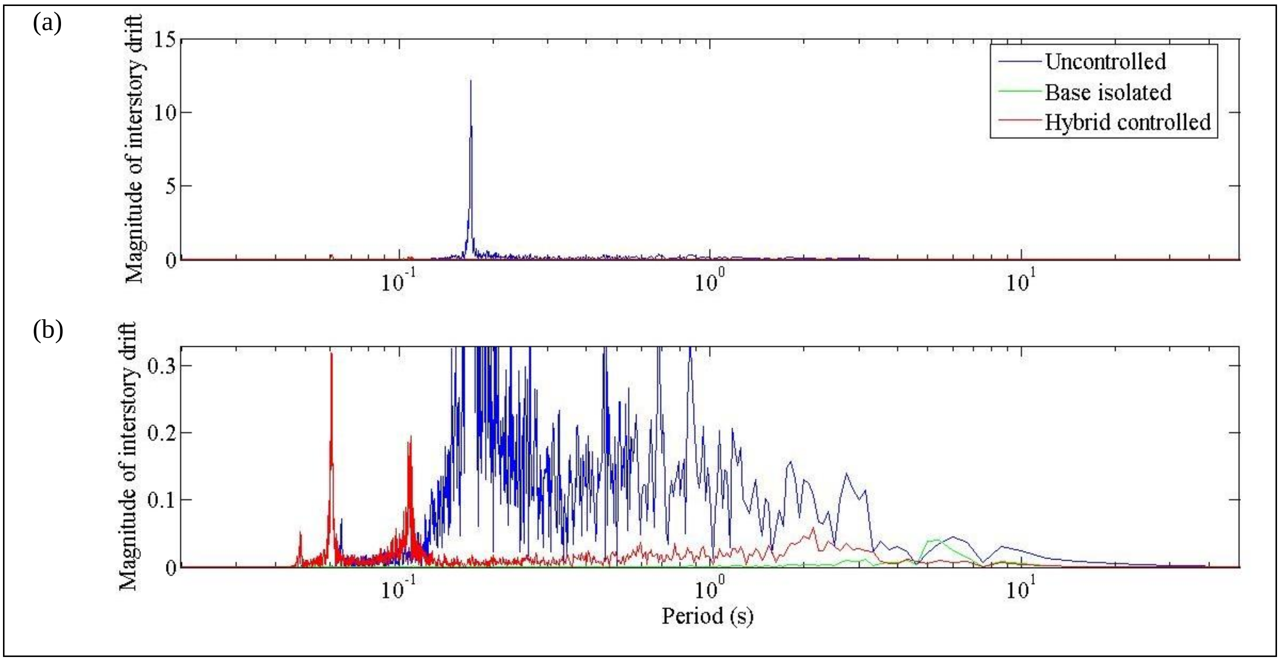

Figure 10. Interstory drift of the third floor in frequency domain ((b) is zoomed in vertical axis)

6. Conclusions

In the present research a base isolated building and a hybrid controlled system which consists of a base isolated building and a MR damper are studied in order to benefit from advantages of both strategies and to avoid the yielding of isolators. The structure's fundamental period is lengthened by adding the base isolator to the bare building. Hence the structure is affected from the smaller components of excitation and is protected from the detrimental effects of earthquake excitation. The advantages of hybrid application of two control systems are revealed. The effectiveness of the control algorithm and the usefulness of MR dampers for response reduction are demonstrated by a numerical earthquake time simulation. The interstory drift reduction of the base is approximately 50% comparing to the response of the base isolated building. Consequently, inclusion of controlled damping in the base level reduces base displacements and velocities, protecting the base isolators from rupture or damage due to large deformations. On the other hand, it increases the building floor responses above the isolators.

7. References

[1] Chandiramani, N.K., "Civil Engineering Applications of Vibration Control (Structural Control) " *Lecture notes*.

[2] Chang, S.P. and Makris, N., 2000. "Effect of Various Energy Dissipation Mechanisms in Supressing Structural Response" *12th WCEE*.

[3] Dyke, S.J., Spencer Jr, B.F., Sain, M.K. and Carlson, J.D., 1996. "Modeling and Control of Magneto-rheological Dampers for Seismic Response Reduction" *Smart Materials and Structures*, Vol. 5(5), pp. 565-576.

[4] Fenves, G.L., Huang, W.H., Whittaker, A.S., Clark, P.W. and Mahin, S.A., 1998. "Modeling and Characterization of Seismic Isolation Bearings" *U.S. Italy Workshop on Seismic Protective Systems for Bridges*.

[5] Hall, J.F., 1999. "Discussion : The role of damping in seismic isolation" *Earthquake Engineering and Structural Dynamics*, Vol.28, pp.1717-1720.

[6] Jansen, L.M., and Dyke, S.J., 1997. "Semi-active Control Strategies for MR Dampers: A Comparative Study" *Intelligent Information Systems*, Vol. 8(10), pp.580-584.

[7] Jung, H.J., Lee, I.W., and Spencer Jr, B.F., 2002. "State-of-the-Art of MR Damper-Based Control Systems in Civil Engineering Applications" *Proceedings of US-Korea Workshop on Smart Infra-Structural Systems*, Korea.

[8] Kelly, J.M., 1999. "The role of damping in seismic isolation" *Earthquake Engineering and Structural Dynamics*, Vol.28, pp.3-20.

[9] Naeim, F., Kelly, J.M., 1999. "Design of Seismic Isolated Structures", John Wiley & Sons Inc., ISBN 0-471-14921-7.

[10] PEER Strong Motion Database, http://peer.berkeley.edu/smcat/ (10/02/2011)

[11] Ribakov, Y., and Gluck, J., 2002. "Selective Controlled Base Isolation System with Magnetorheological Dampers" *Earthquake Engineering and Structural Dynamics*, Vol.31, pp.1301-1324.

[12] Spencer Jr, B.F., Dyke, S.J., Sain, M.K. and Carlson, J.D., 1997. "Phenomenological Model for Magneto-rheological Dampers" *Journal of Engineering Mechanics*, Vol.123(3), pp.230-238.

[13] Soong, T.T., Dargush, G.F., 1999. Design of Seismic Isolated Structures, John Wiley & Sons Inc., ISBN 0-471-96821-8.

[14] Symans, M.D. and S.W. Kelly , 1999. "Fuzzy Logic Control of Bridge Structures Using Intelligent Semi-active Seismic Isolation Systems" *Earthquake Engineering and Structural Dynamics*, Vol.28, pp.37-60.

[15] Yang, G., 2001. **Large-scale Magneto-rheological Fluid Damper for Vibration Mitigation: Modeling, Testing and Control**, PhD Thesis, University of Notre Dame, Notre Dame, Indiana.

[16] Yoshida, O., and Dyke, S.J., 2004. "Seismic Control of a Nonlinear Benchmark Building Using Smart Dampers" *Journal of Engineering Mechanics*, Vol.130(4).